Developmental Biology 360 (2011) 241–255

Contents lists available at SciVerse ScienceDirect

Developmental Biology

journal homepage: www.elsevier.com/developmentalbiology

Genomes and Developmental Control

Identification of a retina-specific *Otx2* enhancer element active in immature developing photoreceptors

Mark M. Emerson, Constance L. Cepko *

Department of Genetics, Department of Ophthamology, Howard Hughes Medical Institute, Harvard Medical School, Boston, MA 02115, USA

ARTICLE INFO

Article history:
Received for publication 25 April 2011
Revised 9 September 2011
Accepted 13 September 2011
Available online 21 September 2011

Keywords:
Retina
Development
Otx2
Specification
Photoreceptors
Enhancer element
Electroporation

ABSTRACT

The homeodomain protein, Otx2, is a critical regulator of vertebrate photoreceptor genesis. However, the genetic elements that define the expression of *Otx2* during photoreceptor development are unknown. Therefore, we sought to identify an *Otx2* enhancer element that functions in photoreceptor development in order to better understand this specification event. Using the technique of electroporation, we tested a number of evolutionarily conserved elements (ECRs) for expression in the developing retina, and identified ECR2 as having robust activity in the retina. We have characterized this element using a number of assays, including Cre-fate mapping experiments. We found that ECR2 recapitulates expression/function of *Otx2* primarily in newly postmitotic photoreceptor cells (PRs), as well as in a subset of retinal progenitor cells (RPCs). ECR2 was also found to be expressed in a subset of horizontal cells (HCs), in keeping with the role of Otx2 in HC development. Furthermore, we determined that the ECR2 element is not active in other Otx2-positive cells such as retinal bipolar cells (BPs), retinal pigmented epithelium (RPE), or the tectum, suggesting that the transcriptional networks controlling *Otx2* expression in these cells are unique from those of developing PRs and HCs. These results reveal a distinct molecular state in dividing retinal cells and their newly postmitotic progeny, and provide genetic access to an early and critical transcriptional node involved in the genesis of vertebrate PRs.

Introduction

The vertebrate retina has been used as a model for studies of the development of the nervous system, including studies on the determination of cell fates. The six classes of retinal neurons and the single retinal glial type arise from multipotent RPCs in a stereotypical order across phylogeny (Livesey and Cepko, 2001). The classes of neurons can be further subdivided into many anatomically and physiologically distinct types of cells, such that more than 50 types of retinal neurons are now recognized (Masland and Raviola, 2000). Many transcription factors have been found to affect the genesis, differentiation and/or survival of one or more retinal cell types. To learn how these factors work together in networks to produce the large variety of retinal cell types will require more sophisticated analyses than simple gain and loss of function experiments. One such type of analysis is the dissection of the cis-regulatory elements of key transcription factors that operate at nodes in networks. The network that controls the production of PRs is a critical one for light sensing tissues, as PRs are the defining cell type for light detection and vision in a wide range of organisms across phylogeny. Elucidation of this network will not only likely reveal the developmental mechanism for production of this cell type, but also may shed some light on the evolution of PRs.

The homeobox transcription factor, *Otx2*, in vertebrates, and the invertebrate homologue, *Otd*, have been established as critical regulators of PR development. In *Drosophila*, *Otd* hypomorphic alleles lead to poor PR development (Vandendries et al., 1996). In mice, conditional removal of *Otx2* in the neural retina leads to loss of PRs, BPs, and HCs. These losses are accompanied by an increase in the number of amacrine cells (ACs) (Koike et al., 2007; Nishida et al., 2003; Sato et al., 2007). Conversely, postnatal viral misexpression of *Otx2* in the rat retina leads to an increase in the number of PRs and the concomitant loss of all other postnatal cell types (Nishida et al., 2003). Furthermore, introduction of *Otx2* into non-neural cells can induce PR gene expression (Akagi et al., 2004; Inoue et al., 2010). Due to the nature of retinal development, with RPCs producing multiple cell classes in overlapping temporal and spatial windows, the actual coincidence of *Otx2* expression with the formation of these cell types during development has not been established. It is likely that there are multiple regulators of *Otx2* expression, operating within different RPC subpopulations and their descendents, offering a window into the transcriptional networks that underlie the generation of multiple cell types within the retina.

The transcriptional control of *Otx2* has been examined previously in several developmental contexts. Enhancer elements for *Otx2* have previously been identified for the anterior neuroectoderm, visceral endoderm, cephalic mesoderm and early eye field (Kimura et al.,

* Corresponding author. Fax: +1 617 432 7595.
E-mail addresses: mark_emerson@hms.harvard.edu (M.M. Emerson), cepko@genetics.med.harvard.edu (C.L. Cepko).

0012-1606/$ – see front matter © 2011 Elsevier Inc. All rights reserved.
doi:10.1016/j.ydbio.2011.09.012

1997; 2000; Kurokawa et al., 2004a; 2004b; Visel et al., 2007). Within the eye, enhancer elements have not been defined beyond the qualitative activity of a very early eye element defined by the Encode project (referred to below as the hs1150 enhancer) (Visel et al., 2007). Expression of Otx2 in the neural retina has been observed in RPCs, retinal ganglion cells (RGCs), adult PRs, BPs, and a subset of Mueller glial cells (MGs) (Baas et al., 2000; Bovolenta et al., 1997; Brzezinski et al., 2010; Fossat et al., 2007; Trimarchi et al., 2008a), though no Otx2 enhancer elements that function in these cells have been described. Therefore, it is currently unknown if *Otx2* expression in the various retinal populations is under the control of a single or multiple transcriptional networks.

As *Otx2* is one of the factors that is expressed in a subset of RPCs, and appears to control specific and multiple cell fates, this study sought to identify enhancers that control its expression. We report here the identification of the Otx2ECR2 element, which directs reporter expression in a subset of the Otx2-dependent cell types of the retina. Otx2-positive RPCs, PR precursor cells and HCs all utilize the ECR2 element, while another Otx2-dependent cell-type, the BP cell, does not. Furthermore this study shows that electroporation can be used to identify meaningful enhancers that track with RPC states in the developing retina, as well as the transitional state from RPC to more mature cell types.

Materials and methods

DNA electroporations: general methodology

The reporter plasmid used was the Stop Tata Enhanced Green Fluorescent Protein Ires Placental Alkaline Phosphatase version 3 (Stagia3) reporter plasmid consisting of a multiple cloning site for insertion of ECRs, a minimal promoter (the TATA box from the thymidine kinase promoter of the herpes simplex virus), and an Enhanced Green Fluorescent Protein, internal ribosomal entry site, and Placental Alkaline Phosphatase (EGFPiresPLAP) reporter cassette (Supplemental Fig. 1A) (Billings et al., 2010). For electroporation experiments in which retinas were to be processed for immunofluorescent detection of the EGFP reporter, a CAG-AU1 coelectroporation plasmid was used to mark electroporated cells (Materials and methods, Supplemental Fig. 1B). This plasmid has a broadly active promoter, CAG (Niwa et al., 1991), which drives the expression of an mRNA encoding an AU1 epitope-tagged Gapdh, which can be detected with immunofluorescence using a monoclonal antibody directed against the AU1 epitope (see below under DNA plasmids). For electroporation experiments in which the PLAP reporter of the Stagia3 plasmid was employed, a CAG-mCherry co-electroporation plasmid was used, which allowed the fluorescence of mCherry to be used as an indication of electroporation efficiency (Supplemental Fig. 1C). For *ex vivo* electroporation (Supplemental Fig. 1D), retinas were placed into an electroporation chamber filled with a mixture of plasmids and voltage pulses were applied to drive the plasmids into retinal cells found in roughly the central 50% of the retina (Step 1, Supplemental Fig. 1D). Retinas were then cultured *ex vivo* on floating filters for 1 to 8 days (Sparrow et al., 1990) (Step 2, 2a Supplemental Fig. 1D). For example, after 2 days *ex vivo*, Otx2-positive cells were scattered throughout the extent of the retina, with the retina tissue still too immature to exhibit distinct or homogeneous layers (Step 2a, Supplemental Fig. 1D). At this stage, some of the Otx2-positive cells would be expected to be RPCs, as assessed by tritiated thymidine labeling preformed previously (Trimarchi et al., 2008b). After 8 days in *ex vivo* culture, the retina had assumed the basic morphological characteristics of the retina with a distinct outer nuclear layer (ONL) where PRs reside, an inner nuclear layer (INL) containing HCs, BPs, ACs, and MGs, and a RGC layer (GCL) containing RGCs and ACs. Otx2 protein was highly expressed in BPs and a small number of MGs in the INL and was relatively weakly expressed in the PRs found in the ONL (Step 2b, Supplemental Fig. 1D). Electroporation of an empty Stagia3 plasmid that had no active enhancer elements showed very little AP activity following histochemical detection compared to one that contains an active enhancer element (Step 3, Supplemental Fig. 1). Immunofluorescent processing of electroporated retinas also allows for the detection of the electroporated population of cells based on AU1 staining and the subsets of cells expressing the EGFP reporter and endogenous proteins such as Otx2 (Step 4, Supplemental Fig. 1).

DNA electroporation: specific methodology

For mouse *ex vivo* electroporation experiments, P0 mouse retinas were dissected in 50% DMEM/50% F12 and then electroporated with typically 200 ng/μl of each plasmid. Electroporations were performed with a BTX Electro Square Porator ECM830 electroporator and a homemade chamber using 5 pulses of 25 V with a pulse length of 50 ms and 950 ms interpulse interval. Chicken *ex vivo* electroporations were performed on embryonic day 5 (E5) retinas with 160 ng/μl of reporter constructs and 100 ng/μl of Cre plasmids, using the same electroporation parameters described for the mouse. Retinas were cultured on 0.2 μm, 13 mm Nuclepore Track-Etch Membrane Whatman filters as reported previously (Kim et al., 2008). After *ex vivo* culture, retinas were taken off the filters and fixed with 4% paraformaldehyde. For electroporated retinas that were to be alkaline phosphatase (AP)-stained, CAG-mCherry was co-electroporated to verify electroporation. A thin border of RPE was left around the ciliary margin as removal of it caused too much damage to the retina. Lens tissue was removed completely after electroporation and before culture. Chicken *in ovo* electroporations were performed on E3 chicks. DNA solution (2.64 μg/μl plasmid Otx2ECR2SF2, 2.19 μg/μl CAG-AU1, 2 μg/μl Fast Green dye) was introduced with a pulled glass needle into the subretinal space of the right eye. A sharp tungsten negative electrode was used to pierce the head region just caudal to the eye and a gold plated electrode was used as a positive electrode anterior to the eye. 10 V pulses were applied for 50 ms for a total of 3 times, 950 ms apart.

DNA plasmids

Due to an inability to completely separate the emission spectra of EGFP and genetically encoded red fluorescent molecules in our paradigm (unpublished observations), an epitope-based co-electroporation plasmid (CAG-AU1) was designed. This allowed the use of a Cy3 fluorescently conjugated secondary antibody that was completely spectrally-segregated from the signal derived by EGFP. The AU1 sequence is a 6 amino acid sequence that can be detected with a specific monoclonal antibody and has been validated to give a good signal-to-noise ratio in the retina (Lim et al., 1990; Shevtsova et al., 2006). To generate a CAG-AU1 plasmid, EGFP was removed from the Stagia3 reporter plasmid and replaced with the mouse Gapdh coding sequence (based on the expressed sequence tag AK164415) that was amplified from adult mouse cDNA. Two copies of the AU1 sequence were placed at the N-terminus of Gapdh (which served only as a carrier protein for the AU1 tags) and separated by glycine residues to give the following protein (MG**DTYRYI**G**DTYRYI**ASvkvgv…) with AU1 peptides shown in bold and Gapdh from the second amino acid shown in lower case. The CAG promoter from CAG-EGFP (Matsuda and Cepko, 2004) was cloned into the Sal1/EcoR1 sites of this AU1Gapdh modified version of Stagia3. No deleterious side effects have been observed by introduction of the CAG-AU1 plasmid into the retina. To generate a Cre responsive AU1 plasmid (CALNL-AU1), the CALNL-EGFP plasmid (Matsuda and Cepko, 2007) was digested with Age1 and BsrG1 to remove the EGFP coding sequence and AU1Gapdh from CAG-AU1 was excised with Age1 and BsrG1 and ligated to the CALNL fragment. A Cre recombinase version of Stagia3 was made by excising EGFP with Age1 and BsrG1, filling in the ends with Klenow polymerase and cloning in a Cre EcoR1/Not1 fragment from CAG-Cre (Matsuda and Cepko, 2007) with ends filled

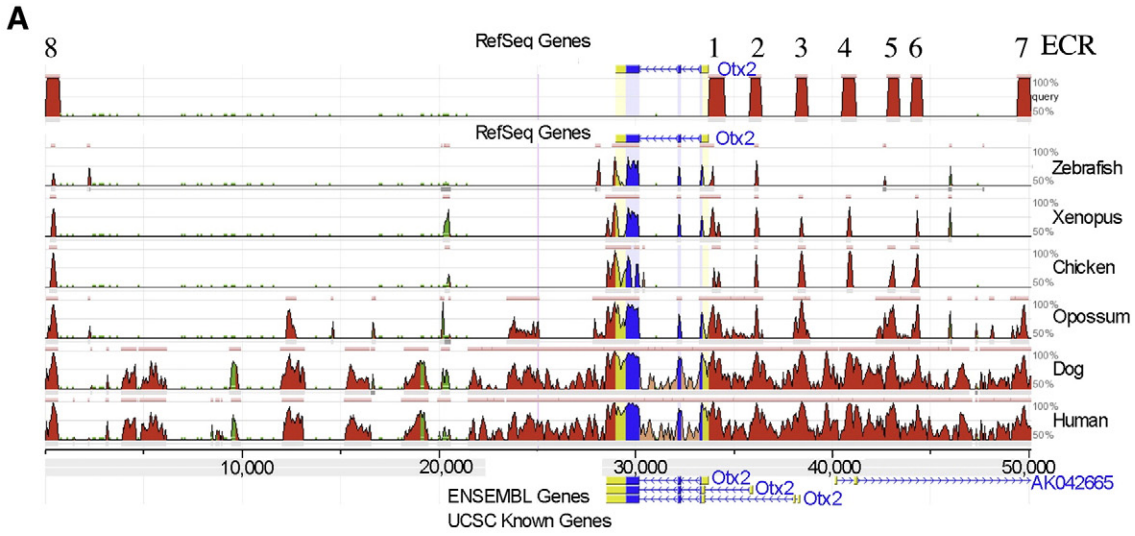

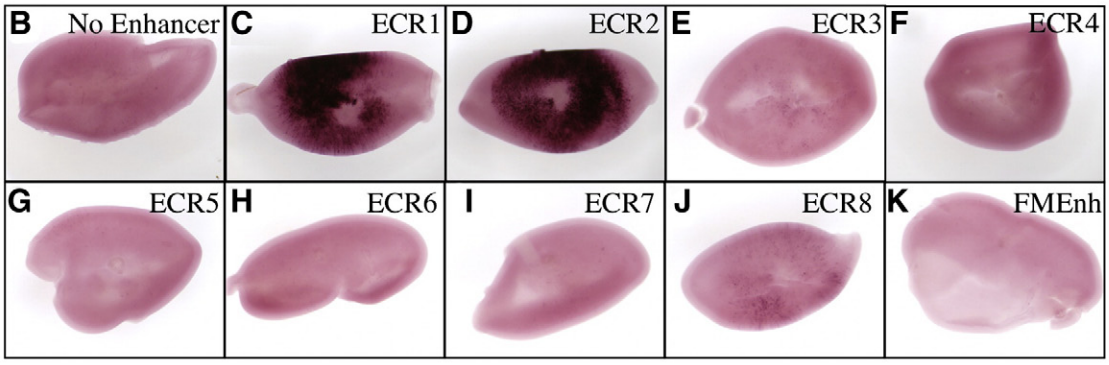

L

Element	MouseP0-P2	ChickenE5-E7	Mouse P0-P8
ECR1	+++	++	++
ECR2	+++	+++	+
ECR3	-	-	-
ECR4	-	-	-
ECR5	-	-	-
ECR6	-	-	-
ECR7	-	-	-
ECR8	+/-	-	-
FM	-	ND	-
hs1150	-	-	-

Fig. 1. Identification and testing of Otx2 ECRs for retinal enhancer activity. (A) Screenshot of the *Otx2* locus generated by the ECR Browser program (see Materials and methods). The three major transcripts of the mouse *Otx2* gene are shown at the bottom with coding sequence shown in blue and untranslated regions shown in yellow. Red peaks correspond to conserved genomic regions found between the mouse reference genome and the genome of species depicted on the right and green peaks are repeat regions. The eight tested ECRs are shown on the top line. ECR1 contains the previously identified cephalic mesenchyme and visceral endoderm enhancers (Kimura et al., 1997; 2000). The previously identified FM enhancer (Kurokawa et al., 2004a) and the element identified by the Encode project (Visel et al., 2007) are located outside of the region depicted. (B–K) Mouse P0 retinas electroporated with reporter constructs for each ECR, cultured for 2 days *ex vivo* and assessed for AP reporter activity. (B) No Enhancer Stagia3 Control reporter vector. (C–J) ECR1-8 in order. (K) Previously identified FM enhancer. (L) Summary of element activity in mouse retinas electroporated at P0 and cultured for either 2 days or 8 days *ex vivo*, and chicken E5 retinas electroporated and cultured for 2 days, and then stained for AP activity. Relative AP activity was assessed by monitoring the amount of electroporation using a co-electroporated CAG-mCherry or CAG-dsRed plasmid and also comparing to retinas electroporated with a No Enhancer Stagia3 control vector. At least two retinas were assayed with each construct and gave similar expression in each case. ND = not determined.

in by Klenow polymerase. *Otx2* ECRs were identified with the ECR browser program (http://ecrbrowser.dcode.org/) and the UCSC Blat server (http://genome.ucsc.edu/cgi-bin/hgBlat). In general, regions conserved in both mouse and chicken were selected, with ECR7 the only exception to this criteria. All of the mouse *Otx2* ECR and enhancer sequences were amplified from genomic sequences using high fidelity Herculase polymerase and PCR-cloned into PGemTeasy. The genomic coordinates of the fragments generated by these amplification reactions can be found in Supplemental Table 1. EcoR1 fragments encompassing these fragments in PGemTeasy were then subcloned into the EcoR1 site of Stagia3. Otx2ECR2 subfragments were generated by PCR (the genomic coordinates of these subfragments are found in Supplemental Table 1), cloned using Sal1/Xho1into Stagia3 to maintain the same orientation as the original OTX2ECR2 fragment, and sequence verified. Alignment of Otx2ECR2 homologs from other species was aligned with the ClustalW program (http://www.genome.jp/tools/clustalw/)

using the default settings and slight adjustments were made by hand to maximize lineup of sequences. A Xho1/Age1 fragment of the bovine rhodopsin promoter (from the pRho-DsRed plasmid described in Matsuda and Cepko, 2004) was subcloned into the Stagia3 plasmid using the same sites. The *Chx10* BP enhancer (see Supplemental Table 1) was amplified from genomic DNA and PCR-cloned into PGemTeasy. As there is an EcoR1 site within this fragment, the larger EcoR1 fragment was subcloned into Stagia3 (digested with Mun1 and EcoR1). The smaller *Chx10* BP EcoR1 fragment was subcloned after this using the non-destroyed EcoR1 site to reconstitute the ECR as it is found in the mouse genome.

Immunofluorescence

Retinas were fixed in 4% paraformaldehyde for 30 min at room temperature, mounted in OCT and 20 μm sections were prepared by cryosection. Blocking was done in 1XPBS plus 0.1% Tween-20 (PBT) and 5% heat-inactivated normal goat serum or donkey serum for 1 h at room temperature. Primary antibodies were applied in block solutions overnight at 4 °C. After three washes with PBT and another block with PBT plus the appropriate serum for 30 min, secondary antibodies in block solution were applied for overnight incubation at 4 °C. Slides were washed three times with PBT and mounted in Fluoromount-G (Southern Biotech). If 4′,6-Diamidino-2-Phenylindole (DAPI) was used, it was applied in the last 15 min PBT wash. Primary antibodies and dilutions used were as follows: chicken anti-GFP (Abcam, ab13970, 1:2000); mouse anti-AU1 (Covance, MMS-130R, 1:2000); rabbit anti-Otx2 (Millipore, AB9566, 1:500); mouse anti-Visinin (DSHB, 7G4 supernatant, 1:250); mouse anti-AP2α (DSHB, 3B5 supernatant, 1:100); rabbit anti-Pax6 (Covance, PRB-278P, 1:500); mouse anti-Pax6 (DSHB, Pax6 supernatant, 1:20); chicken anti-βgalactosidase (Abcam, ab9361, 1:1000); mouse anti-Lim1 + 2 (DSHB, 4F2 concentrated supernatant, 1:30); mouse anti-Brn3a (Millipore, mab1585, 1:400). Appropriate secondary antibodies for multi-labeling were obtained from either Jackson Immunoresearch or Invitrogen.

Imaging and image processing

Confocal imaging was performed with a Leica SP2 inverted confocal microscope using a 40× oil objective, collecting 18 focal planes over 5.7 μm. The four lasers used and their collection windows are as follows: 405 nm laser (410–470 for secondary antibodies; 410–550 for DAPI), 488 nm laser (492–520), 543 nm laser (572–620), 633 nm laser (650–750). Retinas were electroporated in the central 50% of the retina due to orientation within the chamber. Image acquisition occurred anywhere within this area except the extreme periphery of the electroporated patch and the area near the optic nerve head. Imaris software was used to analyze confocal images. Cells were scored manually by examining and annotating individual z-planes for each relevant channel. For all experiments, positive cells were first identified in the channel that represented CAG (AU1 for most figures and βgalactosidase for Fig. 5) and were then scored for the other channels.

Data quantitation and representation

All experiments where percentages of cells were calculated represent the averages calculated from at least three independently electroporated retinas. Typically, an entire field (160 μm × 360 μm) of a section of a retina was scored for the relevant markers and electroporated plasmid reporters. In cases where the particular cells to be scored were less abundant, more than one field of a given retina was examined. Where the particular cells to be scored were very abundant, occasionally less than an entire field was scored. The minimum number of a particular cell type that was scored ranged from 14 to 111 cells per retina, depending on the abundance within the sample, and each percentage shown in the figures was the combined average for three separate retinas. Each graph shows the indicated percentage of cells that were scored for a particular feature, with the types of cells being analyzed for that feature as the denominator (described in the figure legends). For example, in Fig. 3J, out of all of the double AU1-positive/Otx2-positive cells (*i.e.* the denominator) scored in retinas electroporated with the Otx2ECR2 Stagia3 and CAG-AU1 plasmid, 58.4% of these cells were also GFP-positive. Note that different types of cells (different denominators) were used to generate the data in different graphs, as appropriate to the different analyses. Error bars in figures represent the standard error of the mean. In cases where results were tested for statistical significance, a student's *t*-test was applied with a cutoff of $p<0.05$.

Results

Identification of retinal enhancers at the Otx2 locus

During retinal development, Otx2 mRNA and protein expression have been observed in RPE cells, RPCs, newly formed PRs and RGCs, BPs, and a subset of MGs (Baas et al., 2000; Bovolenta et al., 1997; Brzezinski et al., 2010; Fossat et al., 2007; Trimarchi et al., 2008a). To identify potential enhancers of *Otx2* retinal expression, our strategy was to test the ability of ECRs near the *Otx2* locus to activate reporters when introduced into developing retinas. To identify potential novel *Otx2* enhancers, ECRs found in the mouse genome near the *Otx2* locus were identified bioinformatically (see Materials and methods), cloned into the Stagia3 reporter plasmid, and tested for activity in retinal tissue (Fig. 1A). We also tested enhancers that, based on previous work using transgenic mice, were identified as *Otx2* enhancers that direct expression of reporters in specific subdomains of *Otx2* expression. These include expression in the midbrain (the "FM" enhancer) (Kurokawa et al., 2004a), early eye (referred to as the hs1150 enhancer) (Visel et al., 2007), and cephalic mesoderm/ventral endoderm (included in the ECR1 fragment described below) (Kimura et al., 1997; 2000).

As the expression of *Otx2* in PR precursors was of particular interest, given the critical role of *Otx2* in the genesis and/or early phase of PR development (Nishida et al., 2003), the enhancer constructs were tested in both mouse postnatal day 0 (P0) retinas and chicken embryonic day 5 (E5) retinas. These are stages when a large percentage of the postmitotic cells being produced normally become PRs, with the majority of PRs produced in mouse becoming rods (Carter-Dawson and LaVail, 1979) and the majority becoming cones in chick (Morris and Cowan, 1995; Prada et al., 1991). Retinal explants were electroporated *ex vivo*, cultured for two days, and assayed for AP activity. Neither the FM nor the hs1150 enhancer were active in mouse P0 retinas, as the only reporter activity seen was very low, similar to that of the No Enhancer control vector (Fig. 1B, K, L). However, ECR1 (which includes the previously identified cephalic mesoderm and ventral endoderm enhancers) and ECR2 produced robust AP activity, while ECRs 3–8 produced little to no activity above the No Enhancer control vector (Fig. 1B–J, L). Upon sectioning the retinas, it became apparent that, in contrast to a broadly active co-electroporation marker that was expressed in a number of cells, these ECR fragments drove PLAP reporter expression in subsets of cells with distinct morphology and laminar locations. ECR1-positive cells spanned the radial dimension of the retina, with morphology consistent with that of a RPC (Supplemental Fig. 2A, B). However, ECR2-positive cells were located in the developing PR layer and just below, towards the vitreal surface, in a pattern similar to that seen with endogenous *Otx2* (Supplemental Fig. 2C, D, G). A No Enhancer Stagia3 control plasmid did not produce any detectable AP-positive cells among the electroporated cells (Supplemental Fig. 2E, F). In the E5 chicken retina, both ECR1 and ECR2 enhancers were active and the morphologies of positive cells were similar to those observed in the mouse (data not shown). To determine if ECRs 1 and 2 are active in distinct postmitotic retinal

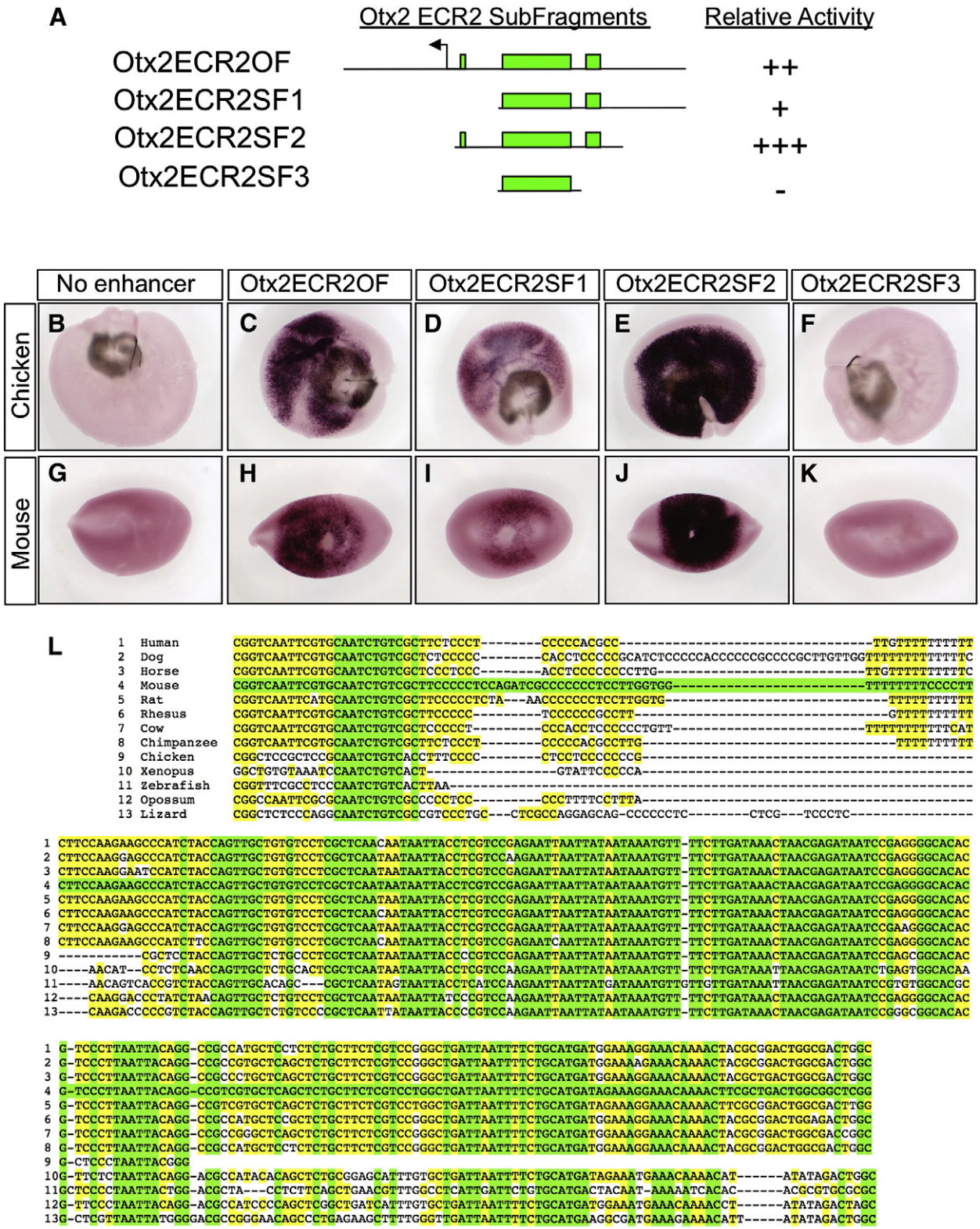

Fig. 2. Generation of a minimal ECR2 element. (A) Schematic of subfragments of ECR2 tested in both P0 mouse retinas and E5 chicken retinas cultured for 2 days *ex vivo*. At least two retinas of each species were tested for each construct and expression was found to be comparable between the biological replicates. The relative activity of each construct compared to the ECR2 original fragment (Otx2ECR2OF) shown in Fig. 2 is indicated by +'s and −'s, with ++ equal to the original. This activity applies to what was observed in both the mouse and the chicken retinas as they were very similar between the two species. Green boxes represent highly conserved blocks. Black arrow (on Otx2ECR2OF) represents identified transcriptional start site and direction of transcription of the genomic Otx2 locus. (B–F) Chicken E5 retinas electroporated and cultured for 2 days *ex vivo* with the identified construct in A. (G–K) Mouse P0 retinas electroporated and cultured for 2 days *ex vivo* with the identified construct in A. (L) Sequences and conservation of the Otx2ECR2SF2 region generated by ClustalW (see Materials and methods). Green shading highlights the mouse ECR2 sequence when 100% conservation of the sequence was found with the 13 depicted species. Yellow shading is used for nucleotide positions that match the mouse, but not in all 12 other species. The chicken genomic sequence was not available for the 3′ end of the ECR2 sequence.

populations, P0 mouse retinas were electroporated and allowed to develop for 8 days *ex vivo*. By this time, almost all of the electroporated retinal cells in the central part of the retina were postmitotic (Young, 1985). ECR1 was expressed in cells resembling MG, while ECR2 was expressed in the PR layer, which has a low level of endogenous *Otx2* expression at this time (Supplemental Fig. 2H–N). All of the other ECRs and previously identified enhancers tested had no expression above background after 8 days *ex vivo* (Fig. 1L). An ECR that controls the relatively strong expression of *Otx2* in BPs was not observed. As the expression of ECR2 correlated with the expression of *Otx2* in newborn PRs and possibly in the RPCs giving rise to them, this enhancer was selected for further study.

Identification of a minimal ECR2 fragment and its conservation across phylogeny

The DNA element that encompasses ECR2 is a 600 base pair fragment with highly conserved blocks of sequence (this original fragment

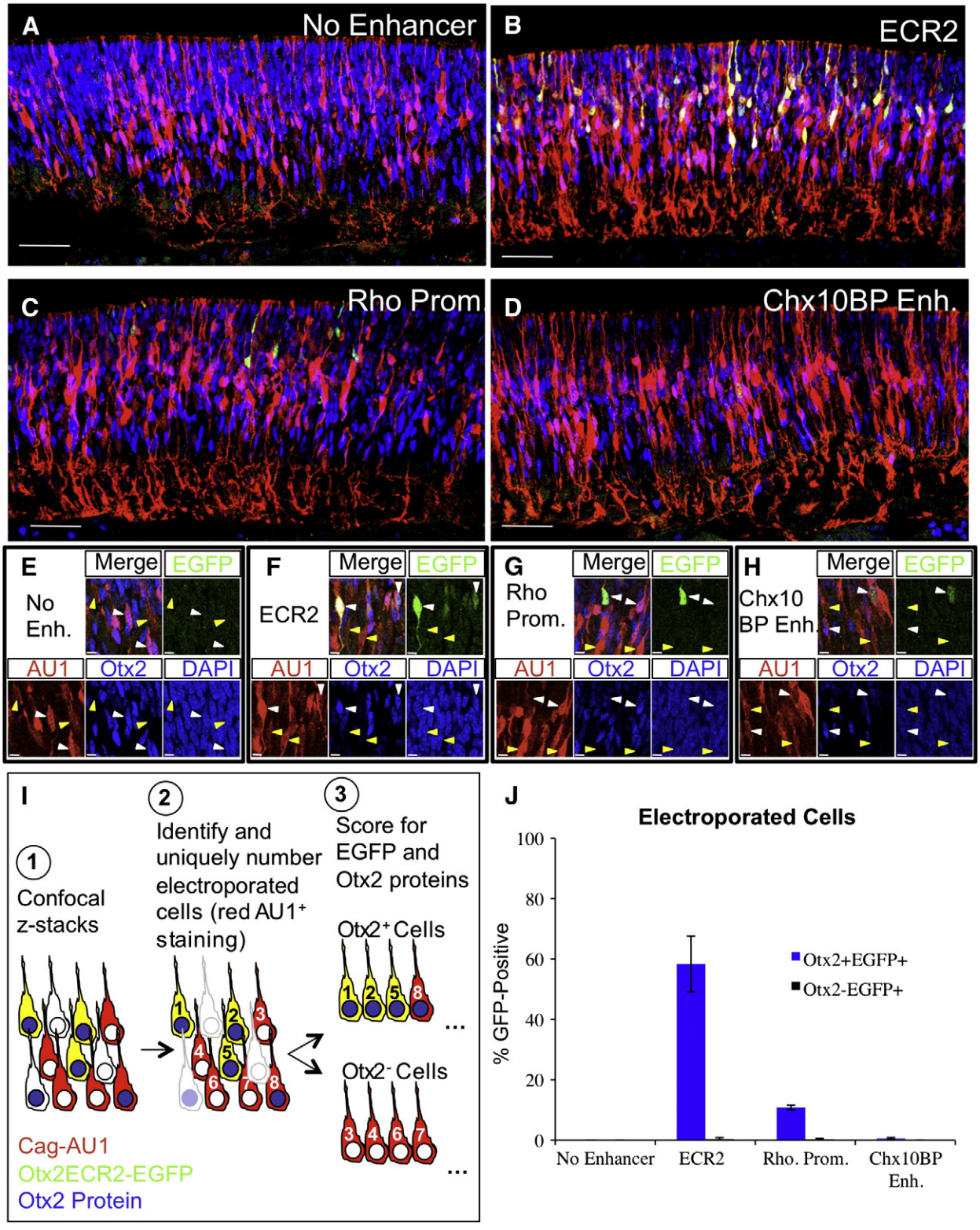

is schematized in Fig. 2A and is referred to as Otx2ECR2OF). Several smaller subfragments encompassing various parts of the phylogenetically conserved blocks within the original enhancer fragment (found in construct Otx2ECR2OF) were then subcloned (Fig. 2A). Each subclone was tested for AP activity in whole mount retinas (Fig. 2B–K). It was observed that inclusion of all of the conserved regions gave the strongest expression of the reporter in both mouse and chick retinas (constructs Otx2ECR2OF and Otx2ECR2SF2, Fig. 2A–K). Furthermore, loss of less conserved regions, including a potential TATA box that could direct transcription in the opposite orientation to that of the reporters, led to an enhancement of reporter expression (Otx2ECR2SF2 *versus* Otx2ECR2OF, Fig. 2, E and J, *versus* C and H). All further experiments and references to ECR2 were carried out with the Otx2ECR2SF2 construct as it was the strongest, most minimal element. Alignment of the Otx2ECR2SF2 sequence revealed strong conservation across vertebrate phylogeny (Fig. 2L).

ECR2 accurately tracks Otx2 positive cells in the developing mouse retina

The retina does not produce different cell types in a spatially restricted manner, or from RPCs dedicated to making only one cell type, with a few exceptions (*e.g.* some types of HCs and possibly PRs) (Godinho et al., 2007; Rompani and Cepko, 2008; Turner and Cepko, 1987). Thus, cells that express a defining cell fate transcription factor can be interspersed among non-expressing cells. To determine if the ECR2 enhancer accurately recapitulated some or all of the *Otx2* expression in the retina, EGFP expression driven by the ECR2 fragment was compared with Otx2 protein expression on a cell-by-cell basis. P0 mouse retinas were co-electroporated with enhancer plasmids driving EGFP and the broadly active CAG-AU1 co-electroporation construct (Supplemental Fig. 1A, B), cultured for 2 days *ex vivo*, and processed for immunofluorescent detection of EGFP, AU1, and Otx2 endogenous protein (Supplemental Fig. 1D). The activity of the ECR2 Stagia3 enhancer plasmid reporter was compared to those of a No Enhancer Stagia3 plasmid (serving as a negative control), a *Rhodopsin* promoter Stagia3 plasmid (driving expression in PR cells; Matsuda and Cepko, 2007) and a *Chx10* enhancer Stagia3 plasmid (driving expression in BP cells; Kim et al., 2008) (Fig. 3A–H).

EGFP and Otx2 colocalization in the electroporated population of cells was analyzed as described in Fig. 3I. While the No Enhancer Stagia3 negative control plasmid failed to label any Otx2-positive cells, the ECR2 element plasmid was capable of labeling almost 60% of the Otx2-positive population (Fig. 3J). In contrast, the *Rhodopsin* promoter was only capable of labeling approximately 11% of the Otx2-positive population, likely representing the relatively small population of PRs generated after the electroporation that had matured to the point of expressing *Rhodopsin* (Fig. 3J) (Morrow et al., 1998). The *Chx10* BP element labeled <1% of the Otx2-positive population, suggesting that either BPs have not been born or that the *Chx10* BP element is not immediately active in newborn BPs (Fig. 3J). In the electroporated Otx2-negative population, very few EGFP-positive cells were detected with the ECR2 fragment, or as expected, for any of the other Stagia3 plasmids (Fig. 3J). The ability of the ECR2 fragment to drive reporter expression in the Otx2-positive population of cells, but not the Otx2-negative population, demonstrates that this element does recapitulate at least some critical aspects of endogenous *Otx2* regulation. It is noteworthy that not all Otx2-positive cells that were electroporated with ECR2-EGFP were positive for EGFP. It is likely that there are other enhancers that drive expression of *Otx2* in this population, such as ECR1. Alternatively, the reporter may not be sensitive enough to capture this expression.

Loss of function mutations of *Otx2* in the mouse leads to a loss of PRs and a large increase in ACs, while overexpression of *Otx2* postnatally causes an increase in PRs and a loss of other postnatally generated cell types, including ACs (Nishida et al., 2003). These experiments suggest that endogenous *Otx2* is unlikely to be expressed in ACs and that ACs should not express ECR2-EGFP. To test if ECR2 was expressed in ACs, mouse P0 retinas were electroporated with ECR2-EGFP and CAG-AU1, cultured *ex vivo* for two days and sections were immunostained and imaged for Otx2, EGFP, AU1, and AP2α (Supplemental Fig. 3A–E). In the mouse retina, AP2α is expressed in a large number of ACs and not at all in mitotic cells (Bassett et al., 2007). In the chicken retina, AP2α is also detected in HCs and we also detect AP2α immunoreactivity in mouse HCs (data not shown) (Fischer et al., 2007). Electroporation at P0 does not target HCs with our protocol (Matsuda and Cepko, 2004) so the only electroporated AP2α-positive cells should be ACs. In order to quantify the overlap of ECR2-EGFP and Otx2 protein with AP2α, a similar counting strategy to that employed for previous experiments was used (Supplemental Fig. 3F). As was expected from the previous genetic data, double immunofluoresence labeling with anti-Otx2 and anti-AP2α showed there were no cells that were both Otx2-positive and AP2α-positive (N>20 electroporated, AP2α-positive cells per retina; 3 retinas scored). When overlap of the enhancer within these same AP2α-positive cells was examined, there were no double-positive cells. This demonstrates that the ECR2 element faithfully represented this aspect of *Otx2* expression.

In order to examine expression of the ECR2 element in more mature retinal cells, explants were allowed to develop for 8 days. By this time, the electroporated portion of the retina was almost completely devoid of cycling cells, as assessed by Ki67 immunoreactivity (data not shown), and as predicted based upon previous studies (Young, 1985).

Fig. 3. The ECR2 element is active in the developing retina. Mouse P0 retinas were co-electroporated with two plasmids (schematized in Supplemental Fig. 1A, B) — the broadly active CAG-AU1 plasmid (to identify electroporated cells) and various Stagia3 reporter plasmids (expressed in a subset of the CAG-AU1 cells). (A–D) Confocal z-stacks of sections through electroporated retinas immunostained for EGFP (green), AU1 (red), Otx2 protein (blue) and DAPI (not shown). The regulatory element present in Stagia3 is identified on each panel. The scleral surface of the retina is at the top of the section. (E–H) Single z-sections of magnified portions of retinas electroporated and immunostained as in the panels A–D. The Stagia3 plasmid used is identified in the upper left portion of the box. The merge panel shows the signal for EGFP (green), AU1 (red) and Otx2 protein (blue) and all other panels represent the signal for the header located above them. White arrows point to electroporated Otx2-positive cells and yellow arrows point to electroporated Otx2-negative cells. (I) Workflow diagram to calculate the percentage of Otx2-positive and Otx2-negative cells that express the EGFP reporter. 1) Confocal z-series were collected for EGFP, AU1, Otx2 protein, and DAPI (not shown). 2) Electroporated cells were identified by positive AU1 staining and each was annotated with a unique number (1 to N). 3) Each cell was scored for two variables — Otx2 protein immunoreactivity and EGFP immunoreactivity. The percentage of cells that were GFP-positive was calculated for the Otx2-positive and Otx2-negative electroporated population of cells and plotted in J (J) Percentage of cells that were EGFP-positive in the Otx2-positive and negative population of electroporated cells for each Stagia3 construct identified along the X-axis. The Otx2-positive population is represented by blue bars and the Otx2-negative population is represented by the black bars. Error bars represent standard error of the mean. Scale bar: 40 μm for A–D. 5 μm for E–H.The ECR2 element is active in the developing retina. Mouse P0 retinas were co-electroporated with two plasmids (schematized in Supplemental Fig. 1A, B) — the broadly active CAG-AU1 plasmid (to identify electroporated cells) and various Stagia3 reporter plasmids (expressed in a subset of the CAG-AU1 cells). (A–D) Confocal z-stacks of sections through electroporated retinas immunostained for EGFP (green), AU1 (red), Otx2 protein (blue) and DAPI (not shown). The regulatory element present in Stagia3 is identified on each panel. The scleral surface of the retina is at the top of the section. (E–H) Single z-sections of magnified portions of retinas electroporated and immunostained as in the panels A–D. The Stagia3 plasmid used is identified in the upper left portion of the box. The merge panel shows the signal for EGFP (green), AU1 (red) and Otx2 protein (blue) and all other panels represent the signal for the header located above them. White arrows point to electroporated Otx2-positive cells and yellow arrows point to electroporated Otx2-negative cells. (I) Workflow diagram to calculate the percentage of Otx2-positive and Otx2-negative cells that express the EGFP reporter. 1) Confocal z-series were collected for EGFP, AU1, Otx2 protein, and DAPI (not shown). 2) Electroporated cells were identified by positive AU1 staining and each was annotated with a unique number (1 to N). 3) Each cell was scored for two variables — Otx2 protein immunoreactivity and EGFP immunoreactivity. The percentage of cells that were GFP-positive was calculated for the Otx2-positive and Otx2-negative electroporated population of cells and plotted in J (J) Percentage of cells that were EGFP-positive in the Otx2-positive and negative population of electroporated cells for each Stagia3 construct identified along the X-axis. The Otx2-positive population is represented by blue bars and the Otx2-negative population is represented by the black bars. Error bars represent standard error of the mean. Scale bar: 40 μm for A–D. 5 μm for E–H.

A proper PR layer was detectable, and more mature cell types, such as BP cells and MG, were morphologically and molecularly identifiable. Analysis of the same four Stagia3 plasmids that were tested after 2 days of *ex vivo* culture, now showed some dramatic qualitative differences in expression when processed identically to those in Fig. 3 (Fig. 4A–H). At this time, Otx2 was expressed weakly in PRs (all of the cells in the ONL), and strongly in a subset of cells in the INL (most of these cells were BP cells and some were a small subset of MG) (Fig. 4I). To quantify these differences, a similar quantitation strategy to that described in Fig. 3I was performed. However, now that PRs could be identified by their position within the section (all of the cells of the ONL), a separate quantitation of electroporated ONL cells was included. Similar to the earlier time point, the No Enhancer Stagia3 control plasmid had very little expression of EGFP in any of the Otx2-positive populations or the Otx2-negative population of the INL, suggesting that there is still only a very small basal transcription rate from this plasmid at this time (Fig. 4A, E, J). In contrast to ECR2-EGFP expression at the earlier time point, there were very few ECR2-EGFP labeled cells in any of the three populations analyzed (Fig. 4B, F, J). What few cells were identifiable as EGFP-positive were present in the ONL PR population, suggesting that either the ECR2 element is very weakly active in these cells or the EGFP may persist from earlier active expression (Fig. 4J). Strikingly, though Otx2 protein is strongly expressed in BP cells, no BP cells were labeled by ECR2-EGFP (Fig. 4J). This suggests that another, yet unidentified, enhancer element must control expression of *Otx2* in BP cells. Despite the lack of labeling of PR and BP cells by ECR2-EGFP, these cell types could be strongly labeled by the Stagia3 plasmids that served as positive controls. The *Rhodopsin* promoter labeled the majority of electroporated PR cells in the ONL, but did not label cells in the INL (Fig. 4C, G, J). Conversely, the *Chx10* BP enhancer strongly labeled Otx2-positive cells in the INL, the vast majority of which are BP cells, but did not label Otx2-positive cells in the ONL or Otx2-negative cells in the INL (Fig. 4D, H, J).

Cre-recombinase driven by the ECR2 element fate maps a significant percentage of PRs, but not ACs or BPs

The EGFP reporter used in previous experiments provides a "real-time expression" readout of the transcriptional activity of an enhancer element within the limitations of the kinetics of EGFP mRNA and protein stability. EGFP reporter expression in a dividing cell may therefore not be detectable in the progeny of that cell (Fig. 5A). In addition, the reporter may be expressed transiently within newly postmitotic cells before they can be identified by cell type-specific antisera (Fig. 5A). A standard fate mapping protocol employing Cre recombinase (Branda and Dymecki, 2004) was thus used to identify both the progeny of ECR2 expressing RPCs and any cell type that transiently expresses the reporter. To this end, we replaced the EGFP coding sequence in the Stagia3 reporter construct with the Cre recombinase coding sequence and co-electroporated ECR2-Cre with the CALNL-AU1 (CAG-LoxP-neo-polyA-LoxP-AU1Gapdh-polyA) Cre reporter. Expression of *Cre* mRNA due to enhancer activity should produce Cre protein, which can excise the neo-polyA cassette of CALNL-AU1. This allows for the production of a mature mRNA molecule that includes the AU1Gapdh marker in all, or almost all cell types, due to the broadly active CAG promoter (Fig. 5B).

We first determined whether AP2α-positive ACs, which do not actively express ECR2-EGFP, have a history of ECR2 activity. To this end, P0 mouse retinas were electroporated *ex vivo* with three plasmids — 1) a CAG-nuclear-βgalactosidase vector to serve as a co-electroporation reporter, 2) the Cre-responsive AU1 reporter (CALNL-AU1) and 3) either a No Enhancer-Cre control plasmid or an ECR2-Cre plasmid as a source of Cre (Fig. 5C). After 2 days of *ex vivo* culture, explant sections were immunostained for βgal, AU1, and AP2α (a specific marker of ACs in electroporated P0 cells) and imaged by confocal microscopy. As the Cre-lox system is known to be extremely sensitive to small amounts of Cre protein, the background level of recombination with the No Enhancer Cre construct was important to determine. However, the No Enhancer Cre plasmid control retinas had very few AU1-positive cells among all of the electroporated cells (Fig. 5D). In contrast, the ECR2-Cre construct produced robust Cre reporter labeling. The majority of cells labeled by this Cre activity were in the upper third of the retina, where the developing PR layer is found (Fig. 5E). The population of electroporated (βgal-positive) AP2α-positive ACs was identified and the percentage of these cells that showed a history of Cre expression (AU1-positive) was quantified (Fig. 5H). Only a small percentage of AP2α-positive ACs was labeled by the ECR2-Cre construct, suggesting that the vast majority of these cells are not generated from cells with a history of ECR2-Cre expression.

In order to assess whether cell types such as PRs and BPs have a history of ECR2-Cre expression, retinas electroporated with the plasmids shown in Fig. 5C were cultured *ex vivo* for 8 days. At this time, PRs and BPs can be easily identified by cell body position (PRs) and expression of markers (BPs). As was seen after 2 days *ex vivo*, 8 days *ex vivo* produced only a few Cre reporter positive cells in retinas that had been electroporated with the No Enhancer-Cre plasmid (Fig. 5F). In contrast, prominent Cre Reporter-positive cells were observed in retinas where the ECR2-Cre plasmid was introduced (Fig. 5G). The percentage of electroporated PRs that were positive for the AU1 Cre reporter in the ECR2-Cre retinas was ~56%, which was significantly more than were labeled by the No Enhancer Cre plasmid (~4%) (Fig. 5I). This suggests that many of the cells labeled by ECR2-EGFP after 2 days *ex vivo* are either cells that divide to give rise to PRs or are themselves newborn PRs.

BPs also require *Otx2* for their genesis and the morphological and molecular features they share with PRs has led to the suggestion that they might be evolutionarily derived from PRs (Arendt, 2003; Lamb et al., 2007). We chose to examine rod BPs (rBPs) due to their abundance and because they can be readily identified as being PKCα-positive and Pax6-negative by immunostaining (some ACs also express PKCα, but are also Pax6-positive). No significant difference in the number of Cre reporter rBPs was observed between the No Enhancer-Cre plasmid and the ECR2-Cre plasmid, suggesting that, unlike PRs, the majority of rBPs do not have a history of ECR2-Cre expression (Fig. 5J).

RPCs and newborn PRs are labeled by ECR2-EGFP in the chicken retina

Given the degree of conservation of the sequences in ECR2, it was of interest to determine if it would have similar activity in the same cell types in disparate species. To this end, the chick retina was electroporated with the mouse ECR2-EGFP Stagia3 reporter at E5 when many of the postmitotic cells being produced would be PRs. After one day *ex vivo*, robust EGFP expression was indeed detected in the chicken retina, with the majority of cells located near the scleral surface of the retina, where most of the Otx2-positive cells also localize (Fig. 6A, B). As was seen in the mouse retina, very good concordance was observed between Otx2 protein expression and ECR2-EGFP reporter expression (Fig. 6C, D). Just as in the mouse, there were some electroporated, Otx2-positive cells that did not turn on the ECR2-EGFP reporter, though this number was smaller, with only about 15% of the electroporated Otx2-positive cells failing to turn on the ECR2-EGFP reporter (Fig. 6C). Unlike the mouse, there was a population, albeit small (~11%), of Otx2 negative cells that did express ECR2-EGFP (Fig. 6D). This could reflect the fact that reporter constructs without any enhancer elements do have some scattered basal expression in the chicken retina, though the percentage of these basal reporter-positive cells is reproducibly very small, <1% (Supplemental Fig. 4, Billings et al., 2010, and data not shown).

It was of interest to determine whether the Otx2-positive cells marked by ECR2 were cycling. We previously reported that *Otx2* RNA could be detected in cycling RPCs, and phenotypic analysis of *Otx2* function is

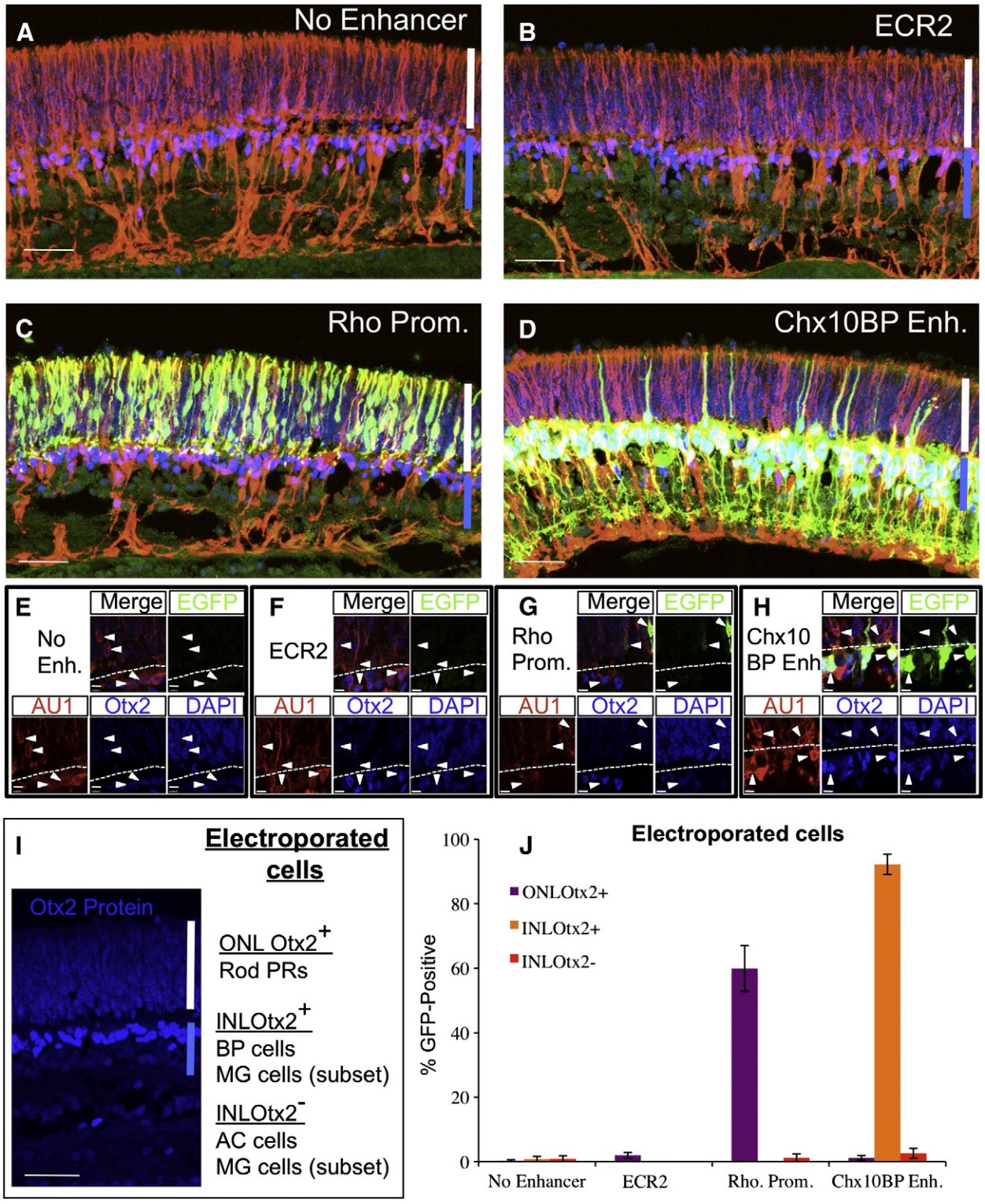

Fig. 4. The ECR2 element is inactive in the retina after mitotic activity is over. Mouse P0 retinas were electroporated with the same plasmids (CAG-AU1 in combination with various Stagia3 reporter constructs) used in Fig. 3, cultured for eight days *ex vivo* and harvested for detection of immunofluorescent reporters. (A–D) Confocal z-stacks of sections through electroporated retinas immunostained for EGFP (green), AU1 (red), Otx2 (blue) and DAPI (not shown). The regulatory element present in Stagia3 is identified on each panel. The extent of the ONL is identified with a white bar and the INL is identified with a blue bar. The scleral surface of the retina is at the top of the section. (E–H) Single z-sections of magnified portions of retinas electroporated and immunostained as in the panels in A–D. The merge panel shows the signal for EGFP (green), AU1 (red) and Otx2 protein (blue) and all other panels represent the signal for the header located above them. White arrows point to electroporated Otx2-protein positive cells. The dotted line demarcates the border between the ONL (located above the line) and the INL (located below the line). (I) A section of a retina immunostained for Otx2 protein (blue) and showing a definitive ONL and INL laminar structure (ONL demarcated by a white bar and INL by a blue bar). The electroporated cells that were found in both the ONL and INL populations are identified by the text to the right of the image. Mouse photoreceptors and bipolar cells have been identified as Otx2-positive and amacrine cells as Otx2-negative by Baas et al., 2000 and a subset of Mueller glia as Otx2-positive by Brzezinski et al., 2010. (J) Quantification of the number of EGFP-positive cells in the population of electroporated cells positive for Otx2 immunoreactivity (Otx2-positive) in the ONL (purple bars) and the INL (orange bars). Also shown is the number of EGFP-positive cells among the electroporated cells negative for Otx2 immunoreactivity (Otx2-negative) in the INL (red bars) for each Stagia3 construct along the X-axis. Otx2 populations in the ONL and the INL were scored separately as they represent distinct cell types. Error bars represent standard error of the mean. Scale bar: 40 μm for A–D. 5 μm for E–H.

consistent with it functioning in RPCs to produce PR fates (Nishida et al., 2003; Trimarchi et al., 2008a). To determine if ECR2-EGFP labels cycling RPCs, the thymidine analog, 5-ethynyl-2′-deoxyuridine (EdU), was used to label cells in S phase. Retinas electroporated with ECR2-EGFP and CAG-AU1 were cultured for 1 day and EdU was applied for 1 h before harvest. Confocal z-stacks of retinal sections were taken after detecting AU1, EGFP, EdU, and Otx2 (Fig. 6E, F). We then examined all of the EGFP-positive cells that were also positive for Otx2 (to make sure none of the "false negative" population observed in Fig. 6D were counted) to determine whether they were EdU-labeled. Indeed, approximately 32% of this population was positive for EdU (Fig. 6G). Since a 1 h pulse of EdU will only label the S phase cells, it is likely that >32% of the ECR2-EGFP labeled cells were cycling, with some of the EGFP-positive cells in other phases of the cell cycle.

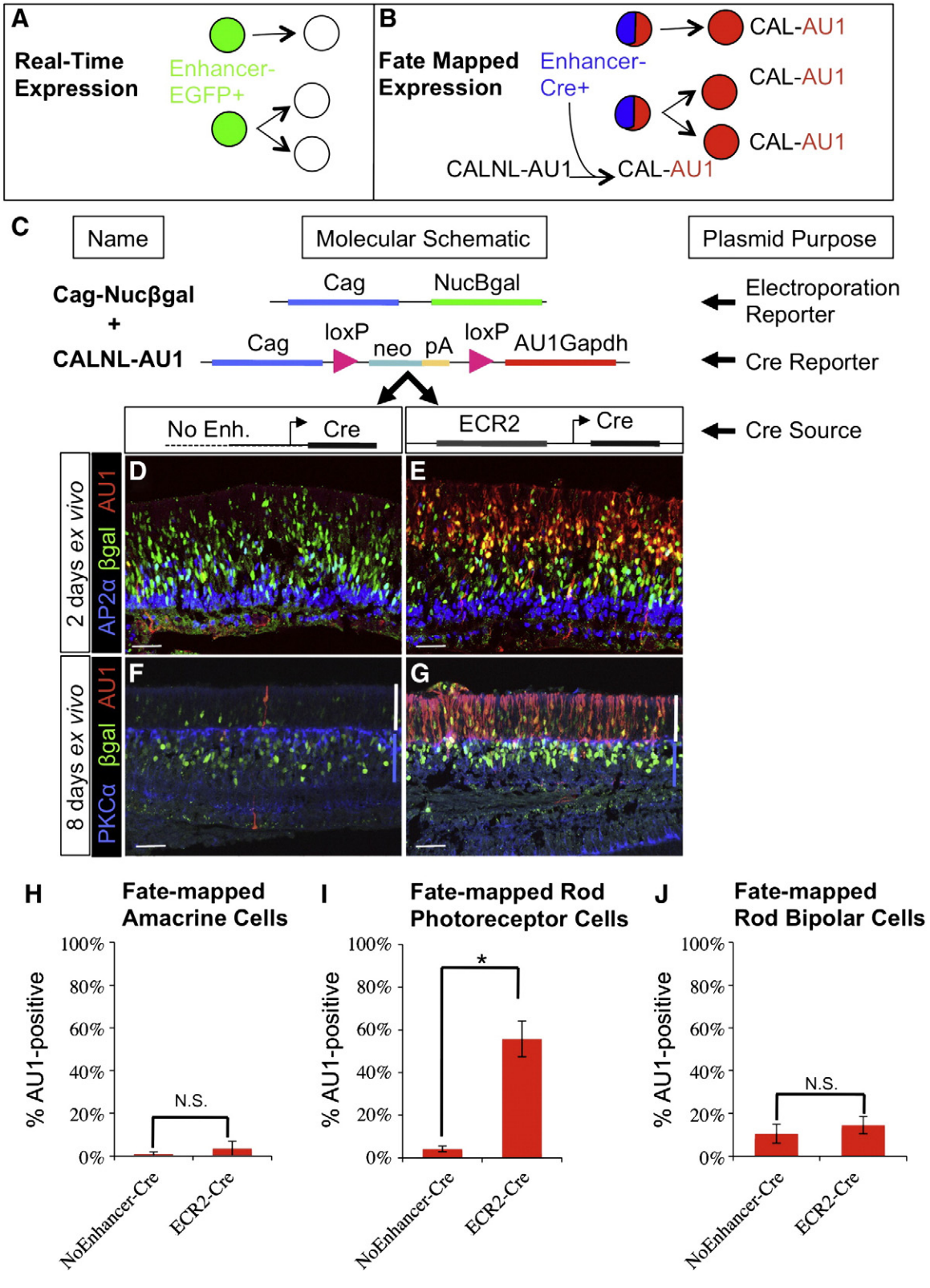

It was of interest to determine if the ECR2 was expressed in early PRs in the chick retina, given the observations of its activity in the mouse retina. We used an exclusive photoreceptor marker at this time point, Visinin (Bruhn and Cepko, 1996; Fischer et al., 2008; Hatakenaka et al., 1985; Yamagata et al., 1990), to identify photoreceptors. When all of the electroporated, Visinin-positive cells were identified it was found that almost 93% of them were also ECR2-EGFP-positive (Fig. 6H–J). This suggests that the vast majority of PRs at this time point either actively express ECR2-EGFP or EGFP mRNA and/or protein persists from expression that occurred in the RPCs that gave rise to the PRs.

In ovo chick retinal electroporations of ECR2-EGFP labels PRs and HCs, but not RGCs

Otx2 is suggested to play a role in both HCs (*Otx2* knockouts lack HCs; Sato et al., 2007) and RGCs (some RGCs transiently express Otx2; Baas et al., 2000). As it is easier to access the early retina in chick embryos than in mouse embryos, we examined *in ovo* electroporated embryonic chick retinas for the expression of ECR2 enhancer activity in HC or RGC. The murine ECR2-EGFP plasmid and a CAG-AU1 plasmid were co-electroporated into stage 18 retinas and harvested three days later (Fig. 7A). Given that *ex vivo*, ECR2 labels the vast majority of electroporated PRs (93%, Fig. 6J), it was expected that PRs would be labeled by the ECR2-EGFP construct *in ovo* as well. When electroporated Visinin-positive cells were scored for EGFP, 72% were indeed positive for EGFP (Fig. 7B, E–H, Q). Interestingly, 30% percent of electroporated HCs (as determined by fluorescent Lim1 immunohistochemistry) were positive for EGFP, despite the fact that almost all of them were negative for Otx2 protein (Fig. 7C, I–L, Q and data not shown). This suggests that the ECR2 enhancer and Otx2 protein are active in RPCs that will give rise to HCs (Liu et al., 2000). Alternatively, the ECR2 reporter is a more sensitive indicator of Otx2 expression in HCs than immunofluorescent labeling for Otx2. In either case, the EGFP may effectively fate map some of the HCs that require *Otx2* for their development. A more definitive Cre recombinase experiment could not be performed as Cre expression appeared to be toxic to the cells of the chicken retina (data not shown). When electroporated RGCs were examined, only about 1% were positive for EGFP (Fig. 7D, M–Q), suggesting that the ECR2 element is not active in RGCs.

The ECR2 element does not recapitulate expression of Otx2 in the tectum or RPE

To determine if the ECR2 enhancer is specific to the retina, the ECR2-EGFP construct was electroporated into developing chicken tectum, which has an endogenous, high expression level of Otx2. Tecta were dissected out of E5 chick embryos and co-electroporated *ex vivo* with reporter plasmids driving EGFP and CAG-AU1 in an identical manner to that done for the retina. Compared to the CAG-EGFP positive control, very few, if any, electroporated Otx2-positive cells were identifiable as EGFP-positive with either the No Enhancer Stagia3 plasmid or with the ECR2-EGFP plasmid (Supplemental Fig. 5A–F; N = 3 tecta for each condition). Thus, ECR2 is incapable of driving reporter expression in a manner that recapitulates the expression of Otx2 in the tectum.

The RPE also expresses a high level of Otx2 and is derived from the optic vesicle, as is the neural retina (Baas et al., 2000). In order to determine if the RPE can utilize the ECR2 enhancer, *in ovo* electroporations were performed to target the RPE of developing chick embryos (see Fig. 7A for how electroporations were performed). Either a negative control (a No Enhancer Stagia3 vector) or the ECR2-EGFP construct was co-electroporated with CAG-AU1 at E3 and embryos were harvested 2 days later. Electroporated RPE cells had no EGFP immunoreactivity with either the No Enhancer Stagia3 plasmid or the ECR2-EGFP Stagia3 plasmid (Supplemental Fig. 5G–J). While not all tissues have been tested, the absence of ECR2 reporter activity in the tectum and RPE suggest that the ECR2 construct exhibits some specificity for neural retina expression.

Discussion

The activity of the ECR2 element correlates with Otx2 protein expression in progenitor cells and newly postmitotic cells

Using the technique of electroporation, this study sought to identify enhancer elements for the Otx2 gene that are involved in photoreceptor development. The expression of EGFP driven by the ECR2 element closely matched that of endogenous Otx2 protein in the developing retinas of both the chicken and the mouse. In both tissues, this labeling was seen at a time when RPCs were present in fair numbers, and cells identified with EGFP often had long processes suggestive of RPCs or migrating precursor cells. Furthermore, in the chicken retina, a one hour S phase labeling paradigm was capable of labeling approximately 30% of cells that were both ECR2-EGFP-positive and Otx2 protein-positive, suggesting that many of these cells were indeed RPCs as has been previously described for endogenous *Otx2* mRNA (Trimarchi et al., 2008a). In the P0 mouse retina electroporated *in vivo*, a small percentage (6.27+/−1.70%) of ECR2-EGFP-positive cells were labeled by EdU after 4 h of EdU labeling (N = 5 retinas, data not shown). Again, this is comparable to the observations made of *Otx2* mRNA-positive cells labeled 4 h after tritiated thymidine introduction in the mouse E18.5 retina (Trimarchi et al., 2008b). These observations demonstrate that the ECR2 element is active in some Otx2-positive RPCs of both the mouse and the chicken, as was seen in assays for endogenous *Otx2* mRNA (Trimarchi et al., 2008a, 2008b). When the activity of the enhancer was assessed at a later time when mitotic activity was almost completely over, the ECR2-EGFP reporter was only found in a very small number of PRs (Fig. 8). EGFP expression controlled by the ECR2 element was thus limited to a developmental time window encompassing cycling RPCs and early postmitotic cells, suggesting that its activity may match that of endogenous *Otx2* in the specification of PRs.

Fig. 5. Fate mapping of cells labeled by Otx2ECR2-Cre. (A) Schematic of an enhancer-EGFP construct showing that transient expression in a precursor cell may not be detectable in the more mature cell or that transient expression in a dividing progenitor cell cannot be detected in the progeny of that cell. (B) Schematic of a fate-mapping experiment where expression of an enhancer-Cre construct (blue) allows conversion of a Cre reporter construct from an inactive form (CALNL-AU1) to an active form (red, CAL-AU1). Transient enhancer activity can indelibly mark all cells that transiently express Cre during their development or that derive from a dividing progenitor cell with Cre expression. (C) Description of the three plasmids used in a fate mapping experiment. CAG-Nucβgal was used as an electroporation marker that expressed nuclear βgalactosidase under the control of the broadly active CAG promoter. CALNL-AU1 is a Cre reporter plasmid that in the unrecombined state has the CAG promoter driving expression of the neo gene. Upon recombination by Cre recombinase, the sequence between the loxP sites is removed and transcription from the CAG promoter now produces transcripts containing the AU1 tag. The third plasmid was the Cre plasmid, which was either a No Enhancer control plasmid (used in D and F) or a plasmid with Cre under the control of the ECR2 element (E and G). (D, E) Confocal z-stacks of P0 mouse retinal sections from retinas that were electroporated with the three indicated plasmids, cultured for two days *ex vivo*, and immunostained for AP2α (blue), βgal (green), AU1 (red) and Otx2 (not shown). The scleral surface of the retina is at the top of the section. (F, G) Confocal z-stacks of P0 mouse retinal sections from retinas that were electroporated with the three indicated plasmids, cultured for eight days *ex vivo* and immunostained for PKCα (blue), Nucβgal (green), AU1 (red), and Pax6 (not shown). The scleral surface of the retina is at the top of the section. (H) Percentage of fate-mapped AP2α-positive ACs found with both the No Enhancer-Cre control plasmid and the ECR2-Cre plasmid after 2 days of *ex vivo* culture. The Y-axis represents the percentage of electroporated AP2α-positive ACs that showed evidence of Cre-mediated recombination. (I) Percentage of electroporated PRs (identified as electroporated cells in the ONL) that showed evidence of Cre-mediated recombination after 8 days of *ex vivo* culture. A significant difference ($p<0.05$, denoted by an *) between the number of PRs fate-mapped with the No Enhancer-Cre control plasmid and the ECR2-Cre plasmid was found when the student's *t*-test was applied. (J) Percentage of fate-mapped rBPs (identified as PKCα+, Pax6-cells) after 8 days of *ex vivo* culture. The Y-axis represents the percentage of electroporated rBPs that showed evidence of Cre-mediated recombination. Error bars represent standard error of the mean. A minimum of three retinas were scored for each construct. N.S. = not significant ($p\geq0.05$). Scale bar: 40 μm.

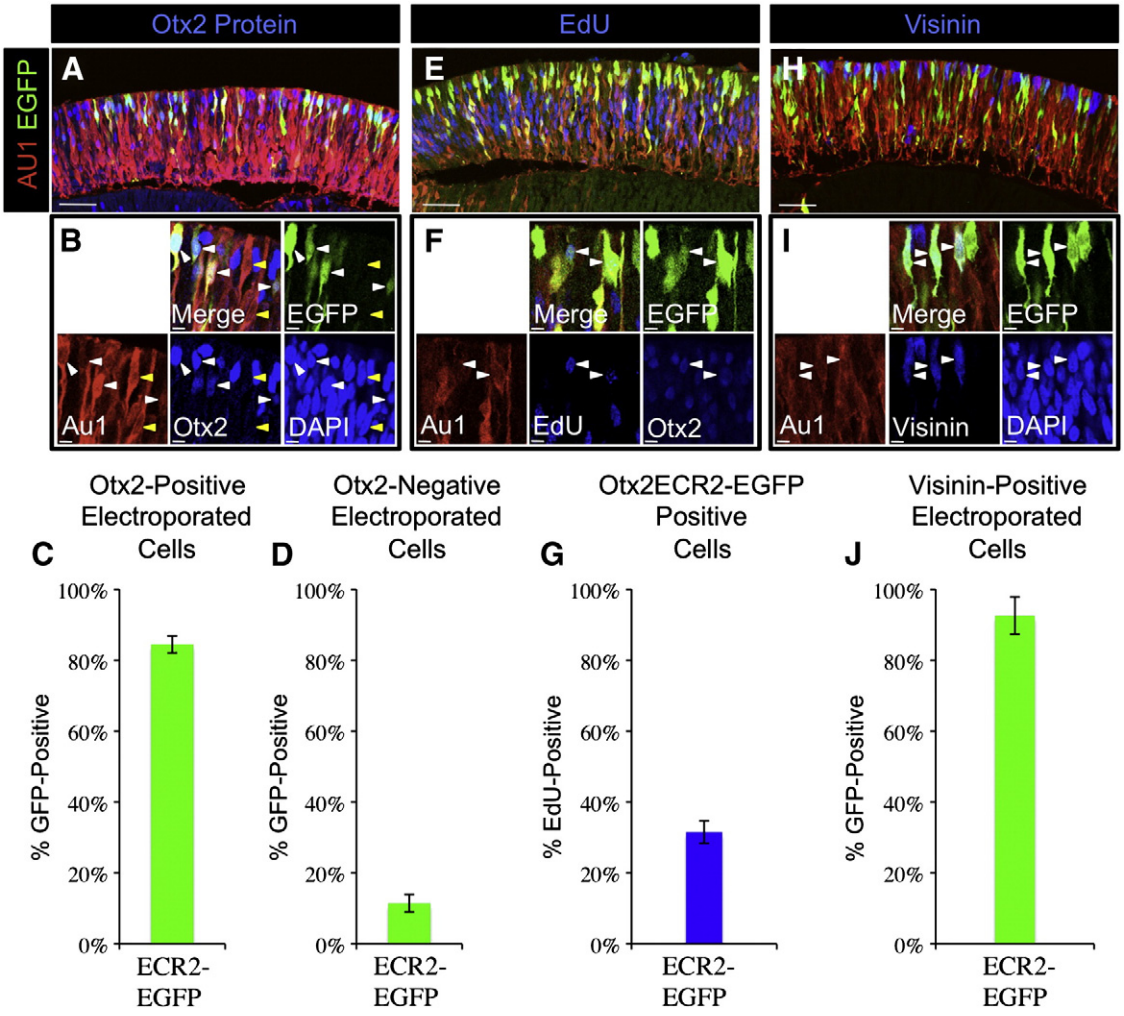

Fig. 6. ECR2-EGFP is expressed in chick RPCs and can be detected in the majority of electroporated chick PRs. Chicken E5 retinas were co-eletroporated with CAG-AU1 and mouse ECR2-EGFP, harvested 2 days later, and immunostained for AU1 (red), and EGFP (green) and other markers (A, B, H, I) or labeled for EdU (E, F). The scleral surface of the retina is at the top of the section. (A) Confocal z-stack of a section immunostained for AU1 (red), EGFP (green), endogenous Otx2 protein (blue), and nuclei visualized with DAPI (not shown). Quantification of these results is shown in C and D. (B) Single z-section of magnified portion of retina electroporated and immunostained as in the panel located just above. The merge panel shows the signal for EGFP (green), AU1 (red) and Otx2 (blue) and all other panels represent the single channel for the marker noted on the panel. White arrows point to electroporated Otx2-positive cells and yellow arrows point to electroporated Otx2-negative cells. (C) Percentage of electroporated Otx2-positive cells that expressed the ECR2-EGFP reporter. The same counting strategy described in Fig. 3I was used for quantitation in C and D. (D) Percentage of electroporated Otx2-negative cells that expressed the ECR2-EGFP reporter. (E) A confocal z-stack of a section from an electroporated retina exposed to a 1 h EdU pulse prior to harvest and then detected for EGFP (green), AU1 (red), EdU (blue) and DAPI (not shown). (F) Single z-section of magnified portion of retina electroporated and immunostained as in the panel located just above. The merge panel shows the signal for EGFP (green), AU1 (red) and EdU (blue) and all other panels represent the single channel for the marker noted on the panel. White arrows point to electroporated GFP-positive/EdU-positive/Otx2-positive cells (G) The percentage of all electroporated, EGFP-positive, Otx2-positive cells also positive for EdU. (H) Confocal z-stack of a section from an electroporated retina immunostained for endogenous Visinin protein (blue), a marker of PRs. AU1 in red and EGFP in green. (I) Single z-section of magnified portion of retina electroporated and immunostained as in the panel located just above. The merge panel shows the signal for EGFP (green), AU1 (red) and Visinin (blue) and all other panels represent the single channel for the marker noted on the panel. White arrows point to electroporated Visinin-positive cells. (J) Percentage of all electroporated Visinin-positive cells that expressed the ECR2 reporter. Error bars represent standard error of the mean. A minimum of three retinas were scored for each condition. Scale bar: 40 μm for A, E and H. 5 μm for B, F and I.

The ECR2 element is active specifically during the development of PRs and HCs

Exploration of the role of *Otx2* in the retina has largely focused on PRs, with evidence suggesting that *Otx2* is both necessary and sufficient for the genesis of PRs (Nishida et al., 2003). Evidence here strongly suggests that the ECR2 fragment is in fact linked with the developmental role of *Otx2* in PR genesis. In the chicken retina, ECR2-EGFP labeled a large number of PRs (as identified by Visinin immunostaining) in both *in ovo* and *in vitro* experiments. When ECR2-Cre was used in a fate mapping experiment in the P0 mouse retina, a significant number of more mature PRs were labeled at a time when they could not be labeled with ECR2-EGFP, suggesting that the ECR2 element is most highly active in the photoreceptor precursor stage. Further studies focused on understanding the regulation of this highly conserved element will shed light on the mechanism by which photoreceptors are specified.

Approximately 30% of HCs were also labeled by ECR2-EGFP when introduced into chicken cells by *in ovo* electroporation. This is in contrast to the fact that the earliest and most specific HC marker examined (Lim1) is not usually coexpressed with Otx2 protein (Emerson and Cepko, unpublished observations). However, it has been documented that conditional removal of *Otx2* leads to loss of HCs suggesting that *Otx2* is expressed at some point in the development of HCs (Sato et al., 2007). The activity of the ECR2 might then suggest that *Otx2* is expressed in early, unidentifiable HCs, and/or the RPC that gives rise to HCs (Fig. 8). However, the majority of HCs were not labeled by ECR2-EGFP. This could be due to heterogeneity among the HCs of the chick (Genis-Galvez et al.,

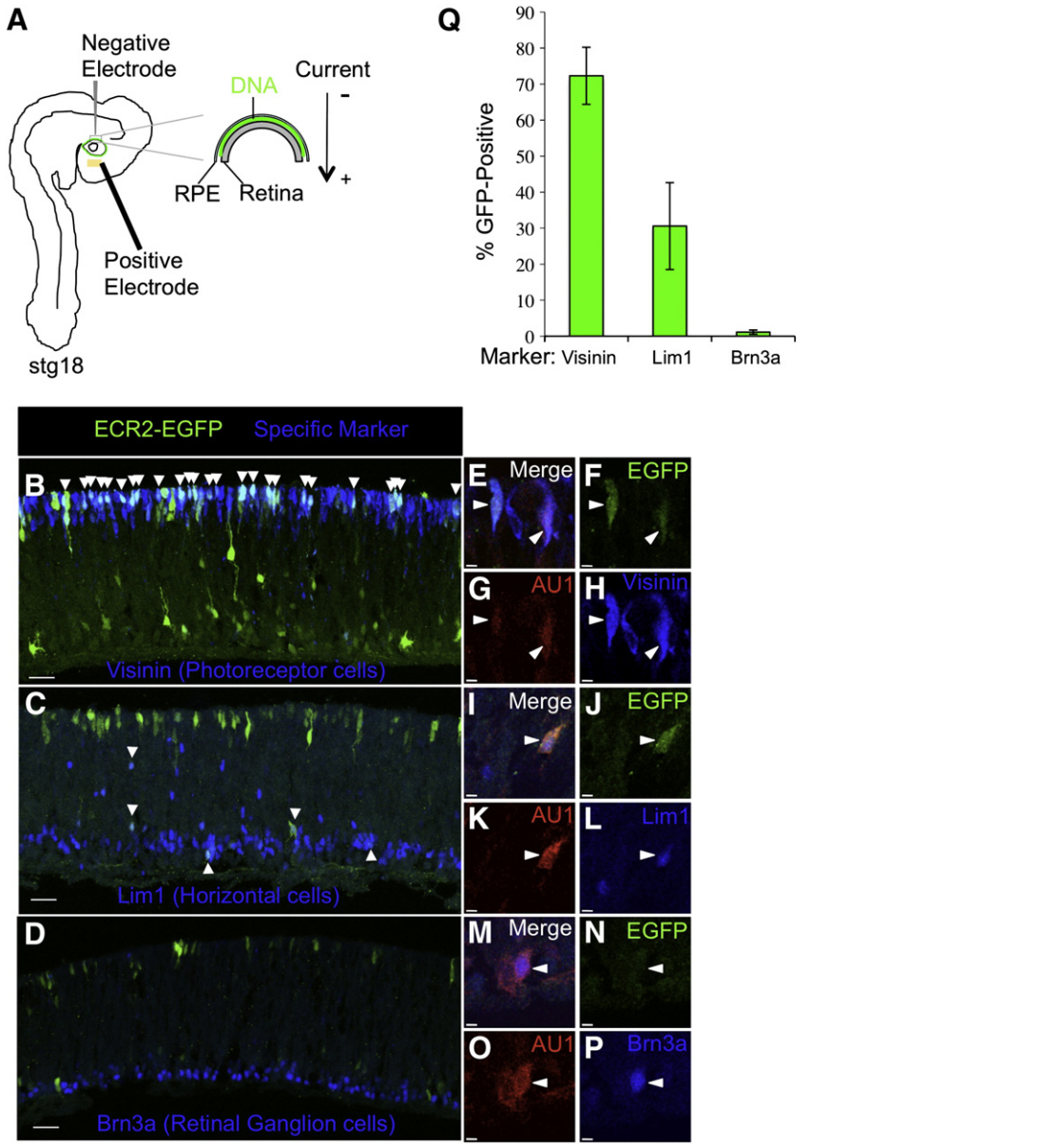

Fig. 7. *In ovo* electroporations of ECR2-EGFP labels PRs and HCs. (A) Schematic of procedure for *in ovo* electroporations using stage 18 (embryonic day 3) chick embryos. After DNA (shown in green) was introduced into the subretinal space using a pulled glass needle, a sharp negative electrode pierced the head of the embryo posterior to the eye and a gold-plated positive electrode was placed anterior to the eye outside of the embryo. Several short pulses of high voltage were applied to move the DNA into developing retinal cells. (B–D) Confocal z-stacks of sections of E6 retinas harvested from embryos electroporated at stage 18. The expression of ECR2-EGFP is shown in green and the expression of cell type-specific markers is shown in blue and is in the following panels: (B) Visinin — PRs (C) Lim1 — HCs (D) Brn3a — RGCs. The scleral surface of the retina is at the top of the section. Arrowheads mark some of the cells with colocalized EGFP reporter expression and the specific marker expression. (E–P) Single z-sections of magnified portions of retinas electroporated and immunostained as in the panel located to the left. The merge panel shows the signal for EGFP (green), AU1 (red) and a cell-type specific marker (blue; E is Visinin, I is Lim1, and M is Brn3a) and all other panels represent the signal identified on the panel. White arrows point to electroporated cells (AU1-positive) also positive for the cell-type specific marker. (Q) Quantitation of the overlap of ECR2-EGFP and various markers in electroporated cells. Electroporated cells were identified by positive AU1 staining (not shown in panels B–D) and for the various markers shown on the X-axis. The percentage of marker-positive, electroporated cells that were also positive for ECR2-EGFP is shown with green bars. Error bars represent standard error of the mean. Three retinas were examined for each marker. Scale bar: 20 μm for B–D. 3 μm for E–P.

1981; Tanabe et al., 2006), wherein some types may not have a history of ECR2 expression. Alternatively, ECR2 activity might occur in an early phase of HC development and we could only detect a fraction of these cells before it was turned off.

In contrast to PRs and HCs, several populations of cells did not have ECR2 activity, demonstrating the specificity of this element. These included cells such as ACs (AP2α-positive ACs of the mouse retina), which do not normally express Otx2 protein (Supplemental Fig. 3). They also included cells that do normally express Otx2, such as rod BPs, RPE cells, and tectal cells. This strongly suggests that the gene networks controlling the regulation of *Otx2* in these cell populations are different from those involved in PRs and HCs. The lack of expression during rBP development is especially interesting given that BP cells and PRs have been suggested to be sister cell types, based on morphological and molecular criteria, which might suggest that they share an *Otx2* transcriptional node (Arendt, 2003; Lamb et al., 2007). In support of this, recent work has shown that loss of the repressor, *Blimp1*, can result in some PRs adopting a BP fate (Brzezinski et al., 2010; Katoh et al., 2010). However, the ECR2 fragment clearly is inactive in BPs, or at least those detected in the 8 day *ex vivo* retina, suggesting that the ECR2 element represents an evolutionary point of divergence between BPs and PRs.

Supplementary materials related to this article can be found online at doi:10.1016/j.ydbio.2011.09.012.

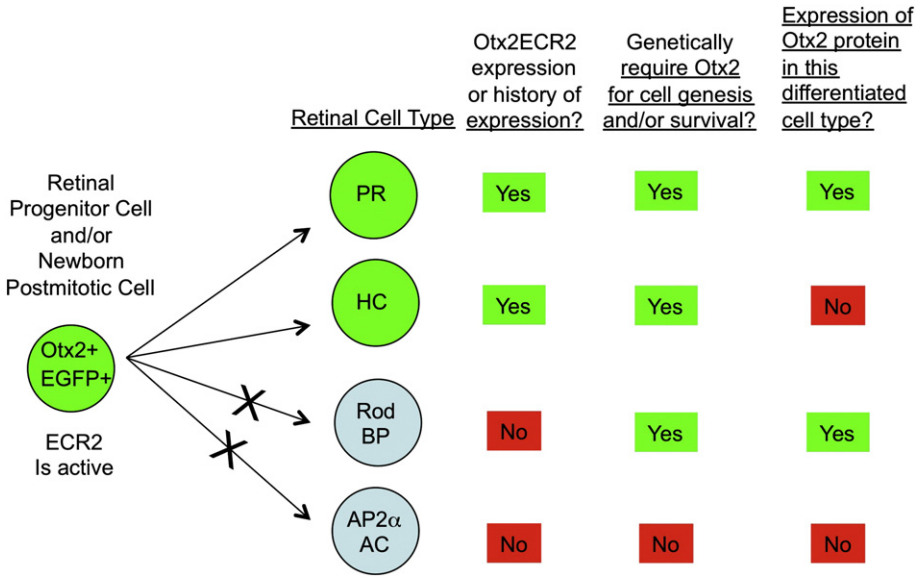

Fig. 8. Summary of the activity of the ECR2 element relative to the known expression and genetic loss-of-function data for Otx2. ECR2-EGFP is active in developing retinas and is strongly correlated with Otx2 protein expression in both chicken and mouse retinas during the period of mitotic activity and neurogenesis. ECR2-EGFP expression and/or ECR2-Cre activity can be localized in PRs, RPCs, as well as in HCs. Both PRs and HCs have been shown to genetically require Otx2 for their production, though HCs do not maintain Otx2 expression throughout their development or in their mature state. rBPs, though they both genetically require (for their maintenance and/or induction) and actively express Otx2 do not have any current or history of ECR2 expression. AP2α-positive ACs, which do not genetically require or actively express Otx2, do not express ECR2, or have a history of its expression.

Acknowledgments

We thank Iain Drummond, Michael Dyer, Julianna LeMieux, and Alan Tenney for critically reading this manuscript. This work was supported by an NIH NRSA-Kirschstein fellowship to M.E. and NIH/NEI grant RO1 EY009676 to C.C. C.C. is an Investigator of the Howard Hughes Medical Institute. The 7G4, 3B5, Pax6, and 4F2 monoclonal antibodies developed by S. Bruhn, T. Williams, A. Kawakami, and T. Jessell/S. Brenner-Morton, respectively, were obtained from the Developmental Studies Hybridoma Bank developed under the auspices of the NICHD and maintained by The University of Iowa, Department of Biology, Iowa City, IA 52242.

References

Akagi, T., Mandai, M., Ooto, S., Hirami, Y., Osakada, F., Kageyama, R., Yoshimura, N., Takahashi, M., 2004. Otx2 homeobox gene induces photoreceptor-specific phenotypes in cells derived from adult iris and ciliary tissue. Invest. Ophthalmol. Vis. Sci. 45, 4570–4575.

Arendt, D., 2003. Evolution of eyes and photoreceptor cell types. Int. J. Dev. Biol. 47, 563–571.

Baas, D., Bumsted, K.M., Martinez, J.A., Vaccarino, F.M., Wikler, K.C., Barnstable, C.J., 2000. The subcellular localization of Otx2 is cell-type specific and developmentally regulated in the mouse retina. Brain Res. Mol. Brain Res. 78, 26–37.

Bassett, E.A., Pontoriero, G.F., Feng, W., Marquardt, T., Fini, M.E., Williams, T., West-Mays, J.A., 2007. Conditional deletion of activating protein 2alpha (AP-2alpha) in the developing retina demonstrates non-cell-autonomous roles for AP-2alpha in optic cup development. Mol. Cell. Biol. 27, 7497–7510.

Billings, N.A., Emerson, M.M., Cepko, C.L., 2010. Analysis of thyroid response element activity during retinal development. PLoS One 5, e13739.

Bovolenta, P., Mallamaci, A., Briata, P., Corte, G., Boncinelli, E., 1997. Implication of OTX2 in pigment epithelium determination and neural retina differentiation. J. Neurosci. 17, 4243–4252.

Branda, C.S., Dymecki, S.M., 2004. Talking about a revolution: the impact of site-specific recombinases on genetic analyses in mice. Dev. Cell 6, 7–28.

Bruhn, S.L., Cepko, C.L., 1996. Development of the pattern of photoreceptors in the chick retina. J. Neurosci. 16, 1430–1439.

Brzezinski, J.A., Lamba, D.A., Reh, T.A., 2010. Blimp1 controls photoreceptor versus bipolar cell fate choice during retinal development. Development 137, 619–629.

Carter-Dawson, L.D., LaVail, M.M., 1979. Rods and cones in the mouse retina. II. Autoradiographic analysis of cell generation using tritiated thymidine. J. Comp. Neurol. 188, 263–272.

Fischer, A.J., Stanke, J.J., Aloisio, G., Hoy, H., Stell, W.K., 2007. Heterogeneity of horizontal cells in the chicken retina. J. Comp. Neurol. 500, 1154–1171.

Fischer, A.J., Foster, S., Scott, M.A., Sherwood, P., 2008. Transient expression of LIM-domain transcription factors is coincident with delayed maturation of photoreceptors in the chicken retina. J. Comp. Neurol. 506, 584–603.

Fossat, N., Le Greneur, C., Béby, F., Vincent, S., Godement, P., Chatelain, G., Lamonerie, T., 2007. A new GFP-tagged line reveals unexpected Otx2 protein localization in retinal photoreceptors. BMC Dev. Biol. 7, 122.

Genis-Galvez, J.M., Garcia-Lomas, V., Prada, F., Armengol, J.A., 1981. Developmental study of axon formation in the horizontal neurons of the retina of the chick embryo. Anat. Embryol. 161, 319–327.

Godinho, L., Williams, P.R., Claassen, Y., Provost, E., Leach, S.D., Kamermans, M., Wong, R.O.L., 2007. Nonapical symmetric divisions underlie horizontal cell layer formation in the developing retina in vivo. Neuron 56, 597–603.

Hatakenaka, S., Kiyama, H., Tohyama, M., Miki, N., 1985. Immunohistochemical localization of chick retinal 24 kdalton protein (visinin) in various vertebrate retinae. Brain Res. 331, 209–215.

Inoue, T., Coles, B.L.K., Dorval, K., Bremner, R., Bessho, Y., Kageyama, R., Hino, S., Matsuoka, M., Craft, C.M., McInnes, R.R., Tremblay, F., Prusky, G.T., van der Kooy, D., 2010. Maximizing functional photoreceptor differentiation from adult human retinal stem cells. Stem Cells 28, 489–500.

Katoh, K., Omori, Y., Onishi, A., Sato, S., Kondo, M., Furukawa, T., 2010. Blimp1 suppresses Chx10 expression in differentiating retinal photoreceptor precursors to ensure proper photoreceptor development. J. Neurosci. 30, 6515–6526.

Kim, D.S., Matsuda, T., Cepko, C.L., 2008. A core paired-type and POU homeodomain-containing transcription factor program drives retinal bipolar cell gene expression. J. Neurosci. 28, 7748–7764.

Kimura, C., Takeda, N., Suzuki, M., Oshimura, M., Aizawa, S., Matsuo, I., 1997. Cis-acting elements conserved between mouse and pufferfish Otx2 genes govern the expression in mesencephalic neural crest cells. Development 124, 3929–3941.

Kimura, C., Yoshinaga, K., Tian, E., Suzuki, M., Aizawa, S., Matsuo, I., 2000. Visceral endoderm mediates forebrain development by suppressing posteriorizing signals. Dev. Biol. 225, 304–321.

Koike, C., Nishida, A., Ueno, S., Saito, H., Sanuki, R., Sato, S., Furukawa, A., Aizawa, S., Matsuo, I., Suzuki, N., Kondo, M., Furukawa, T., 2007. Functional roles of Otx2 transcription factor in postnatal mouse retinal development. Mol. Cell. Biol. 27, 8318–8329.

Kurokawa, D., Kiyonari, H., Nakayama, R., Kimura-Yoshida, C., Matsuo, I., Aizawa, S., 2004a. Regulation of Otx2 expression and its functions in mouse forebrain and midbrain. Development 131, 3319–3331.

Kurokawa, D., Takasaki, N., Kiyonari, H., Nakayama, R., Kimura-Yoshida, C., Matsuo, I., Aizawa, S., 2004b. Regulation of Otx2 expression and its functions in mouse epiblast and anterior neuroectoderm. Development 131, 3307–3317.

Lamb, T.D., Collin, S.P., Pugh, E.N., 2007. Evolution of the vertebrate eye: opsins, photoreceptors, retina and eye cup. Nat. Rev. Neurosci. 8, 960–976.

Lim, P.S., Jenson, A.B., Cowsert, L., Nakai, Y., Lim, L.Y., Jin, X.W., Sundberg, J.P., 1990. Distribution and specific identification of papillomavirus major capsid protein epitopes by immunocytochemistry and epitope scanning of synthetic peptides. J. Infect. Dis. 162, 1263–1269.

Liu, W., Wang, J.H., Xiang, M., 2000. Specific expression of the LIM/homeodomain protein Lim-1 in horizontal cells during retinogenesis. Dev. Dyn. 217, 320–325.

Livesey, F.J., Cepko, C.L., 2001. Vertebrate neural cell-fate determination: lessons from the retina. Nat. Rev. Neurosci. 2, 109–118.

Masland, R.H., Raviola, E., 2000. Confronting complexity: strategies for understanding the microcircuitry of the retina. Annu. Rev. Neurosci. 23, 249–284.
Matsuda, T., Cepko, C.L., 2004. Electroporation and RNA interference in the rodent retina in vivo and in vitro. Proc. Natl. Acad. Sci. U. S. A. 101, 16–22.
Matsuda, T., Cepko, C.L., 2007. Controlled expression of transgenes introduced by in vivo electroporation. Proc. Natl. Acad. Sci. U. S. A. 104, 1027–1032.
Morris, V.B., Cowan, R., 1995. An analysis of the growth of the retinal cell population in embryonic chicks yielding proliferative ratios, numbers of proliferative and non-proliferative cells and cell-cycle times for successive generations of cell cycles. Cell Prolif. 28, 373–391.
Morrow, E.M., Belliveau, M.J., Cepko, C.L., 1998. Two phases of rod photoreceptor differentiation during rat retinal development. J. Neurosci. 18, 3738–3748.
Nishida, A., Furukawa, A., Koike, C., Tano, Y., Aizawa, S., Matsuo, I., Furukawa, T., 2003. Otx2 homeobox gene controls retinal photoreceptor cell fate and pineal gland development. Nat. Neurosci. 6, 1255–1263.
Niwa, H., Yamamura, K., Miyazaki, J., 1991. Efficient selection for high-expression transfectants with a novel eukaryotic vector. Gene 108, 193–199.
Prada, C., Puga, J., Pérez-Méndez, L., López, R., Ramírez, G., 1991. Spatial and temporal patterns of neurogenesis in the chick retina. Eur. J. Neurosci. 3, 559–569.
Rompani, S.B., Cepko, C.L., 2008. Retinal progenitor cells can produce restricted subsets of horizontal cells. Proc. Natl. Acad. Sci. U. S. A. 105, 192–197.
Sato, S., Inoue, T., Terada, K., Matsuo, I., Aizawa, S., Tano, Y., Fujikado, T., Furukawa, T., 2007. Dkk3-Cre BAC transgenic mouse line: a tool for highly efficient gene deletion in retinal progenitor cells. Genesis 45, 502–507.
Shevtsova, Z., Malik, J.M.I., Michel, U., Schöll, U., Bähr, M., Kügler, S., 2006. Evaluation of epitope tags for protein detection after in vivo CNS gene transfer. Eur. J. Neurosci. 23, 1961–1969.
Sparrow, J.R., Hicks, D., Barnstable, C.J., 1990. Cell commitment and differentiation in explants of embryonic rat neural retina. Comparison with the developmental potential of dissociated retina. Brain Res. Dev. Brain Res. 51, 69–84.
Tanabe, K., Takahashi, Y., Sato, Y., Kawakami, K., Takeichi, M., Nakagawa, S., 2006. Cadherin is required for dendritic morphogenesis and synaptic terminal organization of retinal horizontal cells. Development 133, 4085–4096.
Trimarchi, J.M., Harpavat, S., Billings, N.A., Cepko, C.L., 2008a. Thyroid hormone components are expressed in three sequential waves during development of the chick retina. BMC Dev. Biol. 8, 101.
Trimarchi, J.M., Stadler, M.B., Cepko, C.L., 2008b. Individual retinal progenitor cells display extensive heterogeneity of gene expression. PLoS One 3, e1588.
Turner, D.L., Cepko, C.L., 1987. A common progenitor for neurons and glia persists in rat retina late in development. Nature 328, 131–136.
Vandendries, E.R., Johnson, D., Reinke, R., 1996. Orthodenticle is required for photoreceptor cell development in the *Drosophila* eye. Dev. Biol. 173, 243–255.
Visel, A., Minovitsky, S., Dubchak, I., Pennacchio, L.A., 2007. VISTA enhancer browser — a database of tissue-specific human enhancers. Nucleic Acids Res. 35, D88–D92.
Yamagata, K., Goto, K., Kuo, C.H., Kondo, H., Miki, N., 1990. Visinin: a novel calcium binding protein expressed in retinal cone cells. Neuron 4, 469–476.
Young, R.W., 1985. Cell proliferation during postnatal development of the retina in the mouse. Brain Res. 353, 229–239.